Available online at www.sciencedirect.com
SCIENCE DIRECT®
Journal of Chromatography A, 1006 (2003) 3–13
JOURNAL OF CHROMATOGRAPHY A
www.elsevier.com/locate/chroma

Optimal operation of simulated moving bed chromatographic processes by means of simple feedback control

Henning Schramm[a,*], Stefan Grüner[b], Achim Kienle[a,c]

[a]*Max-Planck-Institut Dynamik Komplexer Technischer Systeme, Sandtorstrasse 1, D-39106 Magdeburg, Germany*
[b]*Institut für Systemdynamik und Regelungstechnik Pfaffenwaldring 9, D-70569 Stuttgart, Germany*
[c]*Otto-von-Guericke-Universität Magdeburg, Universitätsplatz 2, D-39106 Magdeburg, Germany*

Abstract

In this contribution, simple methods are presented for controlling a simulated moving bed (SMB) chromatographic process with standard PI (proportional integral) controllers. The first method represents a simple and model-free inferential control scheme which was motivated from common distillation column control. The SMB unit is equipped with UV detectors. The UV signals in the four separation zones of the unit are fixed by four corresponding PI controllers calculating the ratio of liquid and solid flow in the respective separation zone. In order to be able to adjust the product purity a second, model-based control scheme is proposed. It makes use of the nonlinear wave propagation phenomena in the apparatus. The controlled chromatographic unit is automatically working with minimum solvent consumption and maximum feed throughput—without any numerical optimization calculations. This control algorithm can therefore also be applied for fast optimization of SMB processes.

Keywords: Simulated moving bed chromatography; Preparative chromatography; Optimization; Model-based control; Nonlinear wave propagation

1. Introduction

For the production of pharmaceutical compounds or in the area of fine chemistry and biochemistry, chromatographic separation processes have a great importance. Traditionally, chromatographic separations were operated in batch mode. Because of a number of benefits, e.g., lower solvent consumption and lower dilution of the products, nowadays the continuous chromatographic separation using a simulated moving bed (SMB) is increasingly applied to a number of separation problems.

The SMB process (Fig. 1) was patented 4 decades ago by Universal Oil Products [1]. Here, the components of a binary mixture are separated by the use of a simulated countercurrent movement between a liquid solvent and a solid adsorbent phase.

The SMB unit consists of four separation zones bordered by two inlet nodes, feed and solvent and two outlet nodes, extract and raffinate. The movement of the adsorbent phase is simulated by cyclic switching of the inlet and outlet ports in the direction of the fluid flow. If all flow-rates in the unit are chosen properly, the stronger adsorbed component A can be withdrawn at the extract, the less adsorbed

*Corresponding author. Fax: +49-391-6110-543.
E-mail address: schramm@mpi-magdeburg.mpg.de (H. Schramm).

0021-9673/03/$ – see front matter
doi:10.1016/S0021-9673(03)00946-4

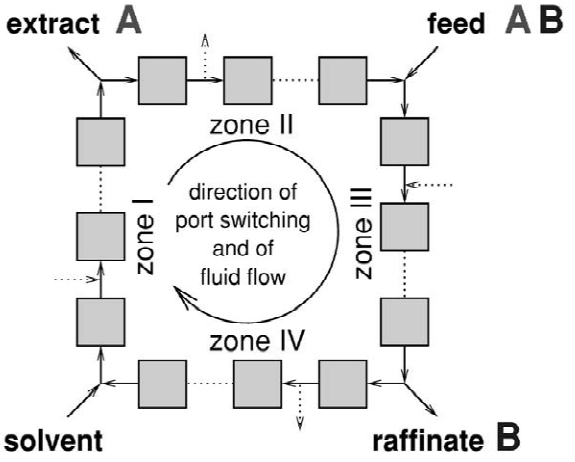

Fig. 1. Simulated moving bed process.

component B appears at the raffinate. For a more detailed description of the SMB process we refer to the literature (e.g., Refs. [2,3]).

For selecting suitable flow-rates a number of methods are available. The well known ''triangle theory'' [3,4] is now common practice to design SMB processes. The key design parameters are the net mass flow-rate ratios m^j, defined as the ratio between liquid and solid flow-rate in each zone j of the unit. For a simplified true moving bed (TMB) unit with true countercurrent flow of liquid and solid phase, the net mass flow-rate ratios can be written as:

$$m^j = \frac{\varepsilon u_j}{(1-\varepsilon)u_s}, \quad j = \text{I, II, III, IV} \tag{1}$$

where ε is the total porosity, u_j the liquid velocity and u_s the solid velocity. For an SMB unit the transport of pore fluid in the direction of the solid phase due to the cyclic switching has to be considered:

$$m^j = \frac{\varepsilon u_j}{(1-\varepsilon)u_s} - \frac{\varepsilon}{(1-\varepsilon)}, \quad j = \text{I, II, III, IV} \tag{2}$$

Here u_s is a fictitious solid velocity which can be calculated from the column length L and the switching time T_s according to:

$$u_s = \frac{L}{T_s} \tag{3}$$

Based on equilibrium theory [5] it is possible to obtain explicit bounds on the flow-rate ratios in each zone. These boundaries can be directly calculated from the adsorption isotherms and the feed concentration. In the m^{II}–m^{III} plane in Fig. 2, different operating regions can be identified for Langmuir type adsorption equilibrium. If flow-rate ratios are chosen, which are lying in the triangle shaped region in the middle of the diagram, complete separation is achieved. From Fig. 2, optimal operating conditions can be easily determined. At point *W*, the difference between m^{II} and m^{III} and therefore the feed throughput is maximized while complete separation is guaranteed. If the conditions for complete separation [3] in the outer zones are fulfilled, minimal solvent consumption is achieved at minimum difference between m^{I} and m^{IV}.

It is obvious, that operating an SMB unit close to this economic optimum causes a high sensitivity to disturbances. Even small fluctuations of the flow-rates or other operating parameters lead to a shift of the operating point into one of the neighboring regions and contaminations of at least one of the product streams occur. This behavior is illustrated in Fig. 3 for a stepwise increase of the feed flow rate by 10%. The figure shows the step response of the concentration profiles in the middle of the switching intervals. The component concentration fronts in zones III and IV move to the right and affect the purity of the product streams. Thus, in order to be

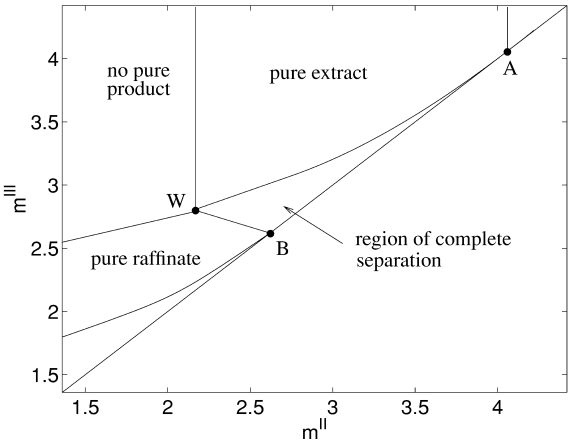

Fig. 2. Different separation regimes determined with triangle theory according to Ref. [3].

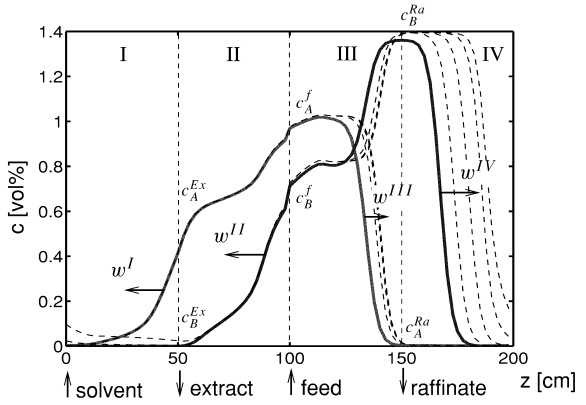

Fig. 3. Step response of the concentration profiles of an SMB unit (middle of switching intervals) operated at minimum solvent consumption and maximum feed throughput for a certain desired product purity (98%). The feed flow-rate was increased by 10%.

able to operate the SMB unit under optimum operating conditions, closed loop control is necessary.

In the literature, some publications dealing with control of SMB processes exist. A number of these contributions uses a model predictive control approach (e.g., Refs. [6–9]). Other control schemes based on input/output linearization are described in Refs. [10] and [11]. Alternatively, two control strategies based on simple PI controllers are presented in this paper. The control strategies are specially tailored to the dynamic characteristics of SMB processes as illustrated in Fig. 3.

The first method represents an inferential control scheme which was motivated by an established technique from distillation column control where the position of concentration fronts in the column is inferred by temperature measurements at specific trays. In the case of a chromatographic separation, these measurements will be UV measurements. No mathematical model is required. The control scheme is useful for rejecting unforeseen disturbances. However since it is an inferential control approach, some offset in the product purity may occur. Nevertheless, this offset is significantly smaller than in the open loop system.

In order to be able to adjust the product purity a second, model-based control scheme is proposed in the second part of the paper. It makes use of the nonlinear wave propagation phenomena in the apparatus. The controlled chromatographic unit is automatically working with minimum solvent consumption and maximum feed throughput—without any numerical optimization calculations. This simple control algorithm can therefore also be applied for fast optimization of SMB processes.

2. Example process

2.1. Modeling

In this contribution, the control algorithms will be verified in a simulation study. For this, the separation of cyclopentanone (component A) and cycloheptanone (component B) is used as an example process. The separation is performed with a preparative scale SMB unit equipped with eight columns (two per zone). The parameters used for the simulation are listed in Table 1.

Table 1
Parameters for the separation of two cycloketones using a preparative-scale SMB unit

Column length (two columns per zone)	25 cm
Column diameter	2.0 cm
Overall void fraction	0.83
Axial dispersion coefficient	D_{ap} (cm^2/min) $= 0.25 \cdot u_j$
Number of theoretical plates per column	50
Feed concentration $c_A^F = c_B^F$	1.25 (%v/v)
Switching time	3.172 min
Langmuir parameter according to Eq. (6)	
a_A	8.52
b_A	0.295 (%v/v)$^{-1}$
a_B	5.97
b_B	0.154 (%v/v)$^{-1}$

The SMB process is modeled using a standard equilibrium dispersive model [5], where c_i is the concentration of component i in the liquid phase and q_i the corresponding solid-phase concentration. The linear fluid velocity is marked by u, z is the spatial coordinate, t the time and ε the total porosity of the column:

$$\frac{\partial c_i}{\partial t} + \frac{1-\varepsilon}{\varepsilon} \cdot \frac{\partial q_i}{\partial t} + u \cdot \frac{\partial c_i}{\partial z} = D_{\mathrm{ap},i} \cdot \frac{\partial^2 c_i}{\partial z^2}, \quad i = \mathrm{A, B} \tag{4}$$

A local equilibrium between the solid and the mobile phases is assumed [i.e., $q_i = q_i(c_A, c_B)$]. The contributions to band broadening due to axial dispersion and mass transfer resistances are lumped into the apparent dispersion coefficients $D_{\mathrm{ap},i}$.

The boundary conditions at the inlet (in) and outlet of the individual columns are given by the Danckwerts relations:

$$D_{\mathrm{ap},i} \left.\frac{\partial c_i}{\partial z}\right|_{z=0} - u(c_i|_{z=0} - c_{i,\mathrm{in}}) = 0,$$
$$D_{\mathrm{ap},i} \left.\frac{\partial c_i}{\partial z}\right|_{z=L} = 0 \tag{5}$$

The adsorption equilibrium can be described using a non stoichiometric Langmuir isotherm:

$$q_i = \frac{a_i c_i}{1 + \sum_{k=\mathrm{A,B}} b_k c_k}, \quad i = \mathrm{A, B} \tag{6}$$

For the simulation of the distributed parameter system a method of lines approach is used. The partial differential Eqs. (4) and (5) are discretized using the finite volume method [12].

2.2. Measurements

The SMB unit is equipped with four UV sensors at different locations in the unit. Two of them are located in the product streams, extract and raffinate and two detectors are situated in the closed circulation loop. UV sensors produce a signal equivalent to the sum of the component concentration. A direct measurement of concentrations is expensive and often not so reliable.

Sensors 3 and 4 in the closed circulation loop are fixed with respect to certain columns and therefore move over the concentration profiles during the switching cycles (Fig. 4). Hence, with these two UV sensors it is possible to obtain a full UV profile after four switches.

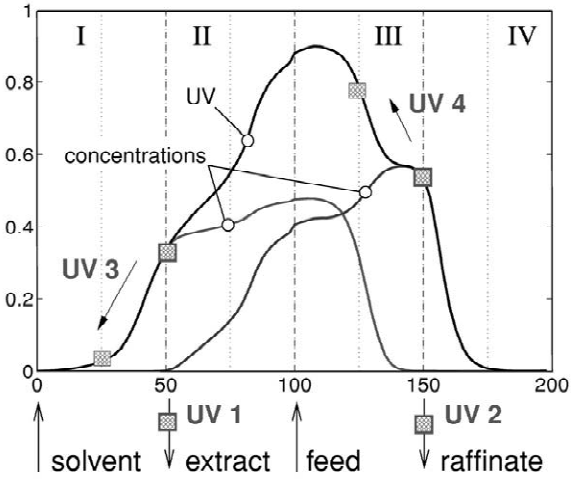

Fig. 4. Sampling of the whole UV profile after a certain number of switches.

The choice of the sensor locations was made as proposed in Ref. [13].

3. Inferential control

The inferential control approach is a very simple way to control a simulated moving bed plant. This technique is well established for the control of distillation columns [14] where the positions of the concentration fronts in the column and therefore product purities are controlled by temperature measurements at specific trays. Replacing the temperature measurements by UV sensors in the middle of the separation zones of a chromatographic SMB unit leads to an inferential control approach for simulated moving bed plants.

The method is illustrated in Fig. 5. The UV profile as sum of the component concentrations in the unit is recorded by the sensors 3 and 4 (Fig. 4) during the operation of the plant. Typically, four different separation fronts can be observed in the concentration as well as in the UV profile. If these fronts are located within different separation zones, they can be fixed by four independent PI controllers.

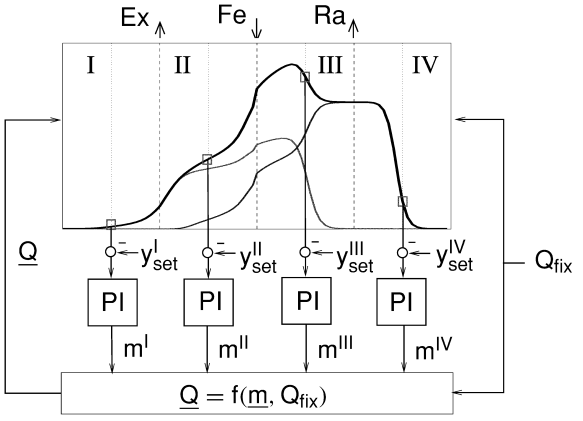

Fig. 5. Inferential control scheme.

During the startup of the SMB unit suitable flow-rates are adjusted according to some design procedure. Subsequently, the plant will be operated open loop until a cyclic steady state is reached. Due to the traveling wave nature of the separation fronts only small adjustments from the optimal operating point are then necessary to position the separation fronts in the middle of the different zones of the unit.

The UV signals in the middle of the separation zones are recorded during the open loop operation of the unit and can subsequently be used as setpoints for the PI controllers. If the cyclic steady state is reached and the product purity at both product outlets fulfill the purity constraints, the controller can be activated. The UV sensors 1 to 4 in the closed circulation loop (Fig. 4) provide measurements for the middle of each separation zone. In the considered example, every four switches a new measurement signal is available for the PI controllers which are located in different zones. Note that the positioning of the PI controllers in the middle of the separation zones implies only weak interaction between the different control loops. The PI controllers can be tuned using a standard SISO (single input, single output) design procedure.

From the difference between measured signals and recorded setpoints, the PI controllers calculate the flow-rate ratios m^j for each separation zone. In a first approach, this comparison will only be done at specific times within a switching interval, e.g., the end of the interval. From the four flow-rate ratios m^j it is now easy to calculate the flow-rates $\underline{Q}$ to control the SMB unit.

There are five degrees of freedom in the plant, therefore it is necessary to fix one flow-rate Q_{fix} in order to be able to calculate the complete set of operating parameters from four m equations. Q_{fix} can be an arbitrary external or internal flow according to the requirements of up- or downstream processes.

In Fig. 6 the SMB unit is operated with optimum flow-rates according to minimum solvent consumption and maximum feed throughput for a desired product purity of 98%. For illustration of the control performance, a step disturbance of the feed flow (10% increase) is introduced to the controlled plant after 20 min. This is the same disturbance as shown in Fig. 3. Contrary to this open loop behavior, the product purity of the controlled unit can be stabilized by a variation of the manipulated variables, i.e., liquid flows. In particular the feed flow-rate returns to its initial value after some transient.

The inferential controller is well suited for keeping an operating point in the presence of flow disturbances. However, a drawback of inferential control is that the product purity is not directly controlled. If the shape of the fronts is changed as a result of a disturbance, the product purity will change, although the controllers adjust the front position such that the difference between measured signal and setpoint is zero.

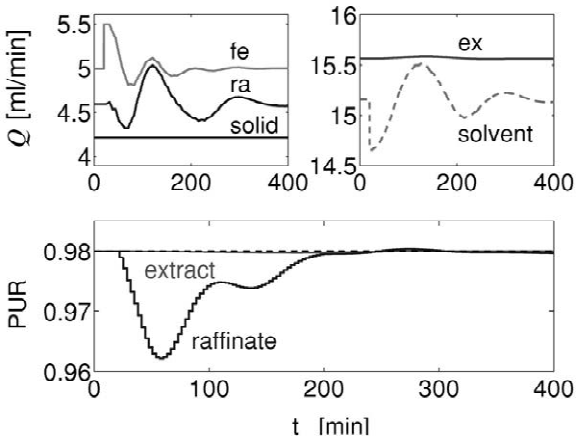

Fig. 6. Step response of manipulated flow-rates and controlled purity after a 10% increase of the feed flow-rate. Inferential control, the switching time was fixed.

The shape of the concentration fronts will vary for example due to a variation of the feed concentration or a change of the adsorption equilibrium in the plant as a result of aging of the stationary phase. Then the controller can not stabilize the purity at its initial value and an offset will appear. This is illustrated in Fig. 7, where a step disturbance of the feed concentration is introduced to the controlled unit. The feed concentration of the weaker adsorbed component is increased by 10%. As expected, the product purity cannot be stabilized at its initial value and an offset is observed. However, the performance of the controlled unit is much better than the performance of the open loop unit. In the corresponding open loop case, the product purity of the extract decreases to about 95% as a result of the disturbance.

Up to now, the measurements have only been evaluated at specific times of the switching intervals. As a result, only a limited amount of information on the dynamics of the concentration fronts is available for the controller which is therefore rather slow. In order to verify this, current investigations are concerned with continuous processing of the measurement signals and using the whole UV profile as measurement for the controller. As a consequence, the setpoints of the PI controllers have to be time variant. First results show a much better control performance. Furthermore, investigations on the application of MIMO (multi input, multi output) control instead of four independent PI controllers will be made.

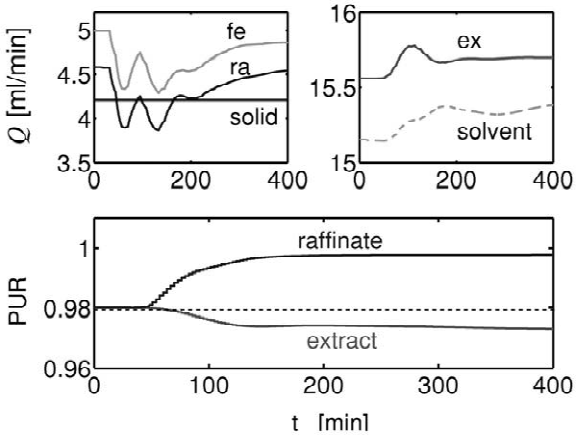

Fig. 7. Step response of manipulated flow-rates and controlled purity after a 10% increase of the feed concentration of the less adsorbed component. Inferential control, the switching time was fixed.

4. Model-based control

In order to be able to adjust the product purity, a second, model-based control scheme was developed. This technique combines a model-based measurement approach with simple PI control. In contrast to the inferential control approach, now the concentration profiles are used to control the unit instead of the UV profile. The concentration profiles are reconstructed online from the UV measurements by a state observer. The fundamentals of the model-based control scheme were also presented in Ref. [15].

The controller is based on the propagation of concentration fronts in the apparatus. According to Ref. [16] the components move through the SMB unit as nonlinear waves. In general, two different kinds of waves are present in the unit: expansive (spreading) waves and constant pattern (shock) waves. In the case of Langmuir type adsorption behavior, spreading waves can be observed in zones I and II and shock waves in zones III and IV. The velocity w of a concentration point $\underline{c}^*$ within a spreading wave can be calculated from:

$$w^j = \frac{Fu_s \cdot \left.\frac{\mathrm{d}q_i(\underline{c})}{\mathrm{d}c_i}\right|_{\underline{c}^*} - u_j}{1 + F \cdot \left.\frac{\mathrm{d}q_i(\underline{c})}{\mathrm{d}c_i}\right|_{\underline{c}^*}}, \quad i = \mathrm{A, B}, \quad j = \mathrm{I, II} \tag{7}$$

with $F = (1 - \varepsilon)/\varepsilon$. The velocity of constant pattern waves follows from:

$$w^j = \frac{Fu_s \cdot \frac{[q_i(\underline{c})]}{[c_i]} - u_j}{1 + F\,\frac{[q_i(\underline{c})]}{[c_i]}}, \quad i = \mathrm{A, B}, \quad j = \mathrm{III, IV} \tag{8}$$

These equations correspond to the equations for an

equivalent true moving bed system, but can also be used for the control of the SMB plant as explained later in this paper. It has to be noted that in the SMB case, all concentration values in Eqs. (7) and (8) represent integral average values over a switching interval. Underlined variables mark a vector of several values or parameters.

The coherence principle of Helfferich and Whitley [17] implies that at a certain spatial point in the unit all component waves travel with the same velocity. Therefore it is sufficient to consider only the velocities of the ''key'' components in every zone (component A in zones I and III and component B in zones II and IV).

Spreading waves are characterized by the fact that lowest concentrations travel with the lowest velocity. Thus, in Eq. (7) the term $\mathrm{d}q_i(\underline{c})/\mathrm{d}c_i\big|_{\underline{c}^*}$ has to be the slope of the isotherm at the left borders of zones I and II, respectively. Provided that the solid and the liquid phase are fully regenerated in the outer zones, the concentrations $\underline{c}^*$ are zero for zone I and $\underline{c}^* = \underline{c}^{\mathrm{Ex}}$ for zone II. In contrast, the quantity $[q_i(\underline{c})]/[c_i]$ in Eq. (8) represents the ratio of the differences between the largest and the smallest concentration of a shock wave, i.e., the height of the shock. With the knowledge of the concentrations $\underline{c}^{\mathrm{f}}$ entering and $\underline{c}^{\mathrm{Ra}}$ leaving zone III (Fig. 3) and the adsorption isotherm, the velocity of the waves in zone III can be calculated. For zone IV the wave velocity results from $\underline{c} = 0$ and the raffinate concentrations $\underline{c}^{\mathrm{Ra}}$ according to complete regeneration of the liquid phase. It has to be noted, that the inlet concentration c_A^{f} of zone III is not necessarily the highest concentration of the wave of component A in zone III. The use of this concentration can therefore cause an error in the calculation of the wave velocity. However, this effect is compensated by the feedback structure of the control algorithm as discussed later in this paper.

With $w^{\mathrm{I}} = w^{\mathrm{IV}} = 0$ and substituting Eq. (1) into Eqs. (7) and (8) the following expressions for the net mass flow-rate ratios in every section of a true moving bed unit can be written:

$$m^{\mathrm{I}} = a_{\mathrm{A}} \tag{9}$$

$$m^{\mathrm{II}} = \frac{\mathrm{d}q_{\mathrm{B}}(\underline{c})}{\mathrm{d}c_{\mathrm{B}}}\bigg|_{\underline{c}^{\mathrm{Ex}}} - \frac{w^{\mathrm{II}}}{Fu_{\mathrm{s}}} \cdot \left(1 + F \cdot \frac{\mathrm{d}q_{\mathrm{B}}(\underline{c})}{\mathrm{d}c_{\mathrm{B}}}\bigg|_{\underline{c}^{\mathrm{Ex}}}\right) \tag{10}$$

$$m^{\mathrm{III}} = \frac{q_{\mathrm{A}}(\underline{c}^{\mathrm{f}}) - q_{\mathrm{A}}(\underline{c}^{\mathrm{Ra}})}{c_{\mathrm{A}}^{\mathrm{f}} - c_{\mathrm{A}}^{\mathrm{Ra}}} - \frac{w^{\mathrm{III}}}{Fu_{\mathrm{s}}} \cdot \left(1 + F \cdot \frac{q_{\mathrm{A}}(\underline{c}^{\mathrm{f}}) - q_{\mathrm{A}}(\underline{c}^{\mathrm{Ra}})}{c_{\mathrm{A}}^{\mathrm{f}} - c_{\mathrm{A}}^{\mathrm{Ra}}}\right) \tag{11}$$

$$m^{\mathrm{IV}} = \frac{q_{\mathrm{B}}^{\mathrm{Ra}}(\underline{c}^{\mathrm{Ra}})}{c_{\mathrm{B}}^{\mathrm{Ra}}} \tag{12}$$

If one flow-rate Q_{fix} is fixed, every other flow $\underline{Q}$ can be calculated from these m values. In order to obtain the correct flow-rates for the SMB case, Eq. (2) has to be used instead of Eq. (1).

For the calculation of the flow-rate ratios m^{I}–m^{IV} according to Eqs. (9)–(12) the concentration values $\underline{c}^{\mathrm{Ex}}$, $\underline{c}^{\mathrm{f}}$ and $\underline{c}^{\mathrm{Ra}}$ are needed. These concentrations are determined online from the available UV measurements by means of a state observer as described in Ref. [18]. Using a process model, the sensor signals of the real plant are simulated. The difference between these simulated and the real measurements, UV 1–4 in Fig. 4, is multiplied by a correction matrix and fed back to the observer model. For a proper design of the correction matrix, the states of the observer model will converge to the real concentration profiles. The state observer consists of an SMB model and provides the cyclic concentration values to the controller. In order to process these concentration values in the control algorithm, the concentrations have to be averaged by integration over a switching interval. Through this, the control task is converted to a simple continuous problem.

It has to be noted, that if the concentrations in the SMB unit can be measured directly (e.g., by a combination of polarimeter and UV detector for enantiomers) no state observer would be needed for the model-based control algorithm.

For the following consideration let us assume that the SMB unit achieves complete separation. If the wave velocities in all zones are zero, the waves are balanced within the zones. If the liquid flow in zones I or II would be slightly decreased, the concentration fronts would start moving to the left until they reach the respective zone boundary. Impurities in the extract outlet or the border to zone IV will occur and complete separation is not achieved. Hence, for complete separation and zero wave velocity minimum liquid flow-rates in zones I and II exist. Analog

considerations can be made for zones III and IV. In these zones, maximum liquid flow-rates are achieved. As a result, the SMB unit is operated with maximum feed throughput and minimum solvent consumption for complete separation.

In most practical applications it is not reasonable to achieve complete separation, lower quality requirements have to be fulfilled. Through this, a more economic operation is possible. For the adjustment of the desired product purity the concentration fronts in zones II and III can be shifted. If the purity at the extract is too low, the fronts in zone II have to be moved to the right, if the purity is too high, the fronts have to be shifted to the left. For the raffinate withdrawal point equivalent instructions can be formulated regarding zone III. The shifting of the wave fronts can be realized by two PI controllers with the product purities as controlled variables, which are adjusted by changing the wave velocities in zones II and III. Then the SMB unit achieves also maximum feed throughput and minimum solvent consumption.

In order to confirm these optimum operating conditions, in Table 2 the optimization of an equivalent TMB unit with parameters according to Table 1 and the model-based controller is compared with a rigorous numerical optimization. The rigorous optimization was performed using the simulation environment Diva [19] with a sequential quadratic programming algorithm. As an objective function, the ratio of solvent and feed flow-rate was minimized corresponding to simultaneous maximization of productivity and minimization of solvent consumption. In order to prevent a breakthrough of component A from zone I into zone IV, the m value in zone I was fixed to the Henry coefficient of component A. This relation follows from the considerations of the triangle theory as well as from Eq. (9). The m values in the remaining three zones were adjusted by the optimization routine as shown in Table 2. Both approaches, rigorous optimization and model-based controller, provide almost the same results for the m values.

For an SMB process the optimal operating parameters will be slightly different [8]. However, it is obvious that also in the SMB case the controller automatically adjusts the corresponding optimal operating conditions due to the feedback principle. In the present case the optimal operating conditions of the SMB process with a product purity of 98% are: $m^{I}=8.520$, $m^{II}=4.823$, $m^{III}=6.010$ and $m^{IV}=4.920$. Here, for the calculation of the flow-rates Q from the m values, Eq. (2) has to be used instead of Eq. (1).

Based on the above considerations, the control structure shown in Fig. 8 was developed. The concentration profiles in the controlled SMB unit are

Table 2
Comparison of rigorous numerical optimization (opt) and optimization using the model-based control algorithm (con) for an equivalent TMB unit (Table 1)

	$PUR_{Ex/Ra}$ (%)	m^{I}	m^{II}	m^{III}	m^{IV}	obj $=Q_{sv}/Q_{fe}$
Triangle theory	100	8.520	4.969	6.072	4.942	
opt	99.5	8.520	5.018	6.084	5.010	3.29
con		8.520	5.017	6.084	5.009	3.29
opt	99.0	8.520	4.904	6.034	4.963	3.15
con		8.520	4.904	6.034	4.958	3.15
opt	98.0	8.520	4.754	5.976	4.902	2.96
con		8.520	4.754	5.975	4.890	2.97
opt	95.0	8.520	4.453	5.891	4.788	2.59
con		8.520	4.453	5.891	4.756	2.62
opt	90.0	8.520	4.109	5.864	4.683	2.19
con		8.520	4.074	5.854	4.599	2.20

The m^{I} value was fixed.

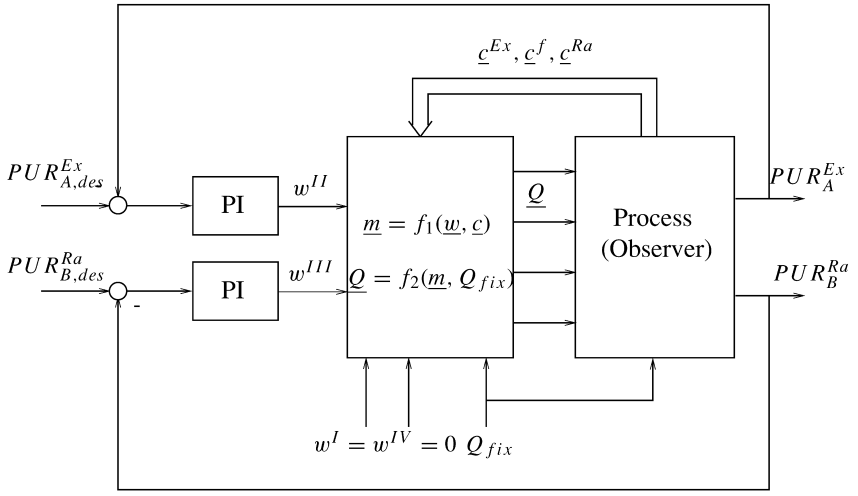

Fig. 8. Model-based control scheme.

determined by the state observer. From the product concentrations the extract and raffinate purity can be calculated and compared with the desired purity. Two independent PI controllers specify the traveling wave velocities in zones II and III, respectively. The four m values are calculated according to Eqs. (9)–(12) by the use of the inflow concentrations to zone III, $\underline{c}^{f}$ and the extract and raffinate concentrations $\underline{c}^{Ex}$ and $\underline{c}^{Ra}$. Complete regeneration of the adsorbent and the liquid phase in zones I and IV is guaranteed. As in the inferential control approach, the flow-rates $\underline{Q}$ can be calculated by fixing an arbitrary flow Q_{fix} from these m values.

In Fig. 9 the time plots of manipulated and controlled variables are shown for a step disturbance of the feed concentration of the less adsorbed component. At 20 min, this concentration was increased by 10%. In the present case the observer and the process model are identical corresponding to an identity observer. Contrary to the inferential control approach (Fig. 7), the model-based controller is able to stabilize the product purity at both outlets at its initial value of 98% without any offset.

Furthermore, the controller can handle setpoint changes of the desired purity. This is illustrated in Fig. 10 where the desired purity of the raffinate outlet is decreased from 98 to 95%. The new purity was adjusted fairly fast by increasing the feed and raffinate flow-rate.

It has to be pointed out, that the flow-rates in every zone of the unit were automatically adjusted such that the unit is operated with minimum solvent consumption and maximum feed throughput. The adjustment of the desired product purity at both product outlets is achieved without any numerical optimization calculation. Therefore, this algorithm is also applicable for fast optimization of SMB processes. For that, the control algorithm can be directly applied to the process model which has to be optimized and no observer is needed.

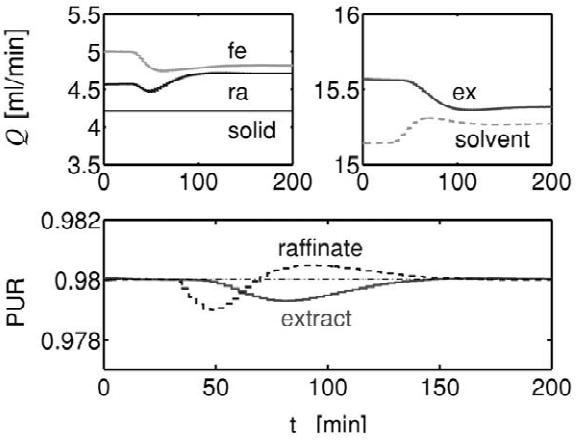

Fig. 9. Manipulated flow-rates and controlled purity after a 10% increase of the feed concentration of the less adsorbed component. Model-based control, identity observer. The switching time was fixed.

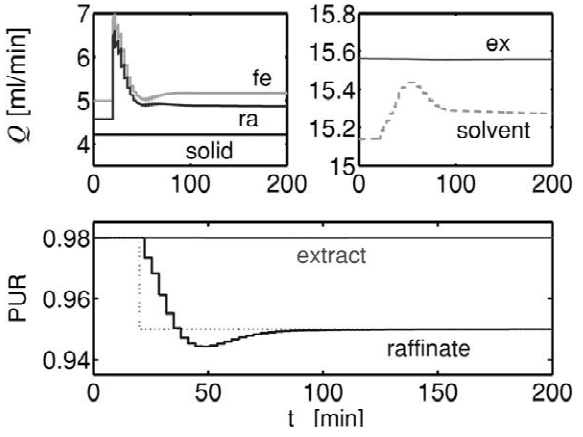

Fig. 10. Manipulated flow-rates and controlled purity after a step change of the desired purity of the raffinate outlet from 98 to 95%. Model-based control, identity observer. The switching time was fixed.

Up to now, the controller works with the assumption of complete regeneration of the adsorbent and liquid phase in the outer zones. Naturally, the controller provides optimum operating conditions for these kind of processes only, where complete regeneration is required. This is fulfilled if a relatively high product purity is demanded.

To complete the considerations about the model-based controller, its behavior in the presence of model inaccuracies has to be discussed. Let us assume in a first step, that we can directly measure the required concentrations without an observer. As shown in the block diagram in Fig. 8, the flow-rate ratios in zones II and III are controlled via feedback control. Therefore inaccuracies of the parameters (e.g., isotherm) of the wave Eqs. (7) and (8) can be tolerated. Eqs. (10) and (11) provide starting values for the m values in the inner zones and these values will be finally adapted by manipulating the wave velocities w^{II} and w^{III} by the PI controllers to the optimum value. In principle, a direct adjustment of the m values or flows as manipulated variables for the PI controllers instead of using the wave velocities is also possible but leads to a decreased robustness of the whole system.

In contrast, the flow-rate ratios in the outer zones I and IV are controlled via feed forward control. The m values in the outer zones are directly calculated from the wave velocity equations. Inaccuracies of the isotherm parameters have influence on the controlled flow-rates in the outer zones. Hence, if the flow-rates in these zones are adjusted by the application of Eqs. (9) and (12), safety factors have to be applied. However, this is also common in the design process of an uncontrolled unit. As an alternative, two additional PI controllers can be applied to the outer zones used to keep the averaged front positions in zones I and IV constant.

For the observer an accurate knowledge of the isotherm parameters is crucial. Here, for model inaccuracies an offset between real and estimated concentration values will appear. This could be a problem if the aging process of the stationary phase is very intense, which is often true for bioseparations. In that case, the concept has to be extended by some suitable measurement or estimation of the adsorbent aging. However, in the considered example of the separation of two cycloketones, aging of the stationary phase is not important and can be neglected.

5. Conclusions

In this paper, two different and relatively simple control schemes for the optimum operation of simulated moving bed processes were presented.

The first method, inferential control, was motivated by common control schemes in distillation. The product purity is inferred from UV measurements at four characteristic positions of the plant. Four independent PI controllers are used to keep these signals constant. The control algorithm does not need any mathematical model and is well suited for processes, where fluctuations of the feed composition can be widely excluded. This is often valid for pharmaceutical separations, where large batches of a raw material are to be processed. For fluctuating feed concentrations an offset in the product purity will appear. However, this offset is much smaller as the deviation appearing from the disturbance in the open loop unit. Aging of the stationary phase will also have this effect on the controlled purity. In this case, an occasional readjustment of the set values for the PI controllers during the operation of the SMB plant seems to be necessary to guarantee a satisfactory operation.

The second, model-based control scheme enables an adjustment of the product purity at both outlet nodes. It combines a model-based measurement technique with simple PI control and makes direct use of the nonlinear wave propagation phenomena in the apparatus. A major advantage of this control algorithm is the automatic adjustment of maximum productivity and minimum solvent consumption for a desired product purity. For a high product purity the optimum operating conditions are adjusted without any numerical optimization calculation—therefore the control scheme is also applicable for fast optimization of SMB processes. This possibility was used for example to investigate a new mode of operation for SMB processes with cyclic modulation of the feed concentration (ModiCon) [20,21].

Of course the model-based control algorithm is only as precise as the observer used to predict the concentration profiles in the unit. Since the only measured quantity remains the UV signal, offsets between predicted and real product purity may occur in the presence of model inaccuracies. Hence, the isotherm parameters have to be determined in advance as accurately as possible.

The simulations in this paper have been performed only for one set of parameters, describing the separation of two cycloketones, cyclopentanone and cycloheptanone. In general, the control algorithms can also be extended to other systems which can not be modeled with Langmuir adsorption isotherms. Application to other systems is an objective for future work.

References

[1] D.B. Broughton, C.G. Gerhold, US Pat. 2 985 589 (1961).
[2] D.M. Ruthven, C.B. Ching, Chem. Eng. Sci. 44 (1989) 1011.
[3] M. Mazzotti, G. Storti, M. Morbidelli, AIChE J. 40 (1994) 1825.
[4] G. Storti, M. Mazzotti, M. Morbidelli, S. Carra, AIChE J. 39 (1993) 471.
[5] G. Guiochon, S.G. Shirazi, A.M. Katti, Fundamentals of Preparative and Non-Linear Chromatography, Academic Press, Boston, MA, 1994, p. 325.
[6] E. Kloppenburg, Ph.D. Thesis, Universität Stuttgart, Stuttgart, 2000.
[7] K.-U. Klatt, F. Hanisch, G. Dünnebier, S. Engell, Comput. Chem. Eng. 24 (2000) 1119.
[8] K.-U. Klatt, F. Hanisch, G. Dünnebier, J. Phys. Chem. 12 (2002) 203.
[9] S. Natarajan, J.H. Lee, Comput. Chem. Eng. 24 (2000) 1127.
[10] E. Kloppenburg, E.-D. Gilles, J. Process Control 9 (1998) 4150.
[11] M. Benthabet, M. Bailly, J.P. Corriou, presented at the AIChE Annual Meeting, Sacramento, CA, 1997.
[12] R. Köhler, K.D. Mohl, H. Schramm, M. Zeitz, A. Kienle, M. Mangold, E. Stein, E.D. Gilles, in: A. Vande Wouwer, Ph. Saucez, W.E. Schiesser (Eds.), Adaptive Method of Lines, Chapman and Hall/CRC Press, New York, 2001, p. 371, Chapter 13.
[13] P. Marteau, G. Hotier, N. Zanier-Szydlowski, A. Aoufi, F. Cansell, Process Control Qual. 6 (1994) 133.
[14] W.L. Luyben, B.D. Tyréus, M.L. Luyben, Plantwide Process Control, McGraw-Hill, New York, 1999.
[15] H. Schramm, S. Grüner, A. Kienle, E.D. Gilles, in: European Control Conference ECC‘01, Porto, 2001.
[16] F.G. Helfferich, P.W. Carr, J. Chromatogr. 629 (1993) 97.
[17] F.G. Helfferich, R.D. Whitley, J. Chromatogr. A 734 (1996) 7.
[18] M. Mangold, G. Lauschke, J. Schaffner, M. Zeitz, E.-D. Gilles, J. Process Control 4 (1994) 163.
[19] M. Mangold, A. Kienle, E.D. Gilles, K.D. Mohl, Chem. Eng. Sci. 55 (2000) 441.
[20] H. Schramm, A. Kienle, M. Kaspereit, A. Seidel-Morgenstern, filed as Pat. DE 102 35 385 9 (2002).
[21] H. Schramm, M. Kaspereit, A. Kienle, A. Seidel-Morgenstern, Chem. Eng. Technol. 25 (2002) 1151.